Summary Report on Work Performed in the Divertor Design Task D308, Subtask 10

Neutronics and Shielding Support Analyses of the ITER Divertor

M.E. Sawan

February 1997

UWFDM-1042

Also ITER/US/96/IV-DV-21.

FUSION TECHNOLOGY INSTITUTE

UNIVERSITY OF WISCONSIN

MADISON WISCONSIN

ITER/US/96/IV-DV-21

Summary Report on Work Performed in the Divertor Design Task D308, Subtask 10

Neutronics and Shielding Support Analyses of the ITER Divertor

Mohamed E. Sawan

Fusion Technology Institute
Department of Nuclear Engineering and Engineering Physics
University of Wisconsin-Madison
1500 Engineering Drive
Madison, WI 53706

February 1997

UWFDM-1042

Executive Summary

During the year 1996, the US home team performed neutronics and shielding analyses as part of the divertor design task D308. The design of ITER has been evolving during the EDA phase. The latest design is the interim design and has been driven by the need to simplify assembly, maintenance, and manufacturing, and to reduce costs. A main feature of the design is the use of 20 toroidal field (TF) cased coils. The design utilizes 60 divertor cassettes with vertical targets and a central dome. Knowledge of nuclear heating and radiation damage levels in the different components of the divertor cassette is essential for proper design analysis. Twenty large divertor ports are utilized for assembly and disassembly of the divertor cassettes and for vacuum pumping. Radiation streaming into these ports can produce excessive heating and damage the TF coils in the divertor region. Reducing nuclear heating and radiation damage in the TF coils to acceptable levels particularly in the regions behind the divertor cassettes and adjacent to the large divertor ports is an important shielding issue. Radiation damage to parts of the vacuum vessel in the divertor region need to be quantified to assess the feasibility of rewelding. Due to the geometrical complexity of the divertor region, three-dimensional analyses are required. This design subtask (subtask 10) is aimed at modeling the ITER divertor region for three-dimensional Monte Carlo, determining the neutron wall loading distribution, and performing three-dimensional neutronics and shielding calculations for the divertor region to determine the nuclear parameters in the divertor cassette and surrounding vacuum vessel and TF coils. This report summarizes the work performed and the results obtained in this design subtask during the year 1996.

The detailed geometrical configuration of the divertor cassette has been modeled for 3-D neutronics calculations. The model includes one and a half cassettes with the associated 1 cm gaps between adjacent cassettes. The model includes in detail the high heat flux plasma facing components (PFC), the vertical targets, the wings with associated plates, the gas boxes, as well as the central dome and cassette bodies. The divertor pumping duct at the bottom of each cassette as well as the rails upon which the cassettes move toroidally during maintenance are also included. The cassette model is divided into 32 cells to allow determination of the detailed

spatial variation of nuclear parameters in the cassette. The divertor cassette model has been integrated with the general ITER model that includes detailed modeling of the first wall, blanket with associated coolant manifolds and back plates, VV, TF coils, central solenoid, and PF coils with all toroidal and poloidal gaps. The major vacuum vessel penetrations are included in the model. This includes the divertor port at the bottom of the reactor. The port wall is 20 cm thick and is cooled by 20% water. No additional shielding is included around the port.

The source neutrons are sampled from the source distribution in the ITER plasma. The MCNP code was modified to sample source neutrons from the pointwise source distribution in the ITER plasma provided numerically by the San Diego JCT at 1600 mesh points. The poloidal distribution of the neutron wall loading in the different regions of ITER has been determined. For the nominal 1500 MW fusion power, the peak neutron wall loading in the divertor region is 0.6 MW/m^2 at the divertor cassette dome.

The neutronics parameters have been calculated in the different components of the divertor cassette. These parameters included nuclear heating, atomic displacement and helium production. The radiation damage was calculated for both stainless steel and copper structures. The largest heating and damage occurs in the dome PFC which has a full view of the plasma and has the largest neutron wall loading. The peak nuclear heating is 10.75 W/cm^3. In general, the nuclear parameters in the inboard side of the cassette are lower than those in the outboard side that has a larger view of the plasma. The total nuclear heating has been calculated for the 60 divertor cassettes to be 102.4 MW. The major contributors are the outer vertical target with 23.1 MW and the dome PFC with 19.7 MW.

The peak helium production in the VV behind the pumping ducts is 0.5 He appm/FPY implying that rewelding might be feasible. In addition, helium production in the divertor port wall is less than 0.04 He appm/FPY. The TF coils are well protected from radiation streaming into the divertor ports with the peak end-of-life insulator dose, neutron fluence, and Cu damage being well below the design limits. The total nuclear heating in the parts of the TF coils in the divertor region is only 2.1 kW. Heating in the remainder of the coils including contribution from streaming in other major ports needs to be determined to calculate the total magnet heating.

1. Introduction

The divertor cassette design went through several changes to improve its performance. Neutronics and shielding features were considered for the design variations. The Interim ITER design utilizes 60 divertor cassettes with vertical targets and a central dome. Knowledge of nuclear heating and radiation damage levels in the different components of the divertor cassette is essential for proper design analysis. 20 large divertor ports are utilized for assembly and disassembly of the divertor cassettes and for vacuum pumping. Radiation streaming into these ports can produce excessive heating and damage in the TF coils in the divertor region. Reducing nuclear heating and radiation damage in the TF coils to acceptable levels particularly in the regions behind the divertor cassettes and adjacent to the large divertor ports is an important shielding issue. Radiation damage to parts of the vacuum vessel (VV) in the divertor region need to be quantified to assess the feasibility of rewelding. Due to the geometrical complexity of the divertor region, three-dimensional (3-D) analyses are required.

2. Three-Dimensional Calculational Model

Due to the geometrical complexity of the divertor region, 3-D models are required to properly determine the nuclear parameters. 3-D neutron-gamma transport calculations have been performed for the divertor region. The continuous energy, coupled neutron-gamma-ray Monte Carlo code MCNP-4A [1] has been used. The nuclear data used is based on the most recent FENDL-1 evaluation [2]. The detailed geometrical configuration of the divertor cassette has been modeled for 3-D neutronics calculations. The drawings provided by the Joint Central Team (JCT) at Garching for the interim ITER design are the basis for the 3-D modeling. The model represents a nine degree toroidal sector of ITER. Hence, it includes one and a half cassettes with the associated 1 cm gaps between adjacent cassettes. The model includes in detail the high heat flux plasma facing components (PFC), the vertical targets, the wings with associated plates, the gas boxes, as well as the central dome and cassette bodies. The 37.5 cm wide and 17.5 cm thick divertor pumping duct at the bottom of each cassette is included in the model. The rails upon

which the cassettes move toroidally during maintenance are also included. The cassette model is divided into 32 cells to allow determination of the detailed spatial variation of nuclear parameters in the cassette. Figure 1 shows a vertical cross section of the cassette model at a toroidal location at the center of the cassette through the pumping ducts. Figure 2 gives the cells used in the MCNP calculations to determine the spatial distribution of the nuclear parameters.

The divertor cassette model has been integrated with the general ITER model. The integrated model includes detailed modeling of the first wall, blanket with associated coolant manifolds and back plates, VV, TF coils, central solenoid, and PF coils. All toroidal and poloidal gaps between adjacent blanket modules are included. The major vacuum vessel penetrations are included in the model. This includes the divertor port at the bottom of the reactor. Due to symmetry, only 1/40 of the reactor is modeled with surrounding reflecting boundaries. The model includes half a TF coil and half a divertor port. The divertor port is 254.5 cm high with a width increasing from 97 cm at the bottom to 176 cm at the top. The port wall is 20 cm thick and is assumed to consist of 80% 316SS and 20% water. No additional shielding is included around the port. The TF coils are segmented to determine the nuclear heating and damage in the parts adjacent to the port resulting from radiation streaming.

The output of the MCNP geometry plotting routine given in Figs. 3 and 4 show vertical cross sections through the TF coil and the middle of the vacuum vessel ports, respectively. The detailed reactor geometrical modeling is illustrated. Figure 5 is a horizontal cross section at z = -6 m in the middle of the divertor port. The divertor pumping ducts in the divertor cassettes are shown in this figure. Also shown is the part of the TF coil adjacent to the divertor port. A coil case which is about 20 cm thick surrounds the winding pack. Several additional surfaces have been added in the divertor region to allow use of geometry splitting with Russian Roulette variance reduction techniques employed in MCNP to improve the accuracy of the calculated nuclear responses.

A combination of cones, tori, cylinders, and planes was utilized for accurate modeling of the geometry. A total of 475 surfaces has been used in the model, of which 164 are fourth degree

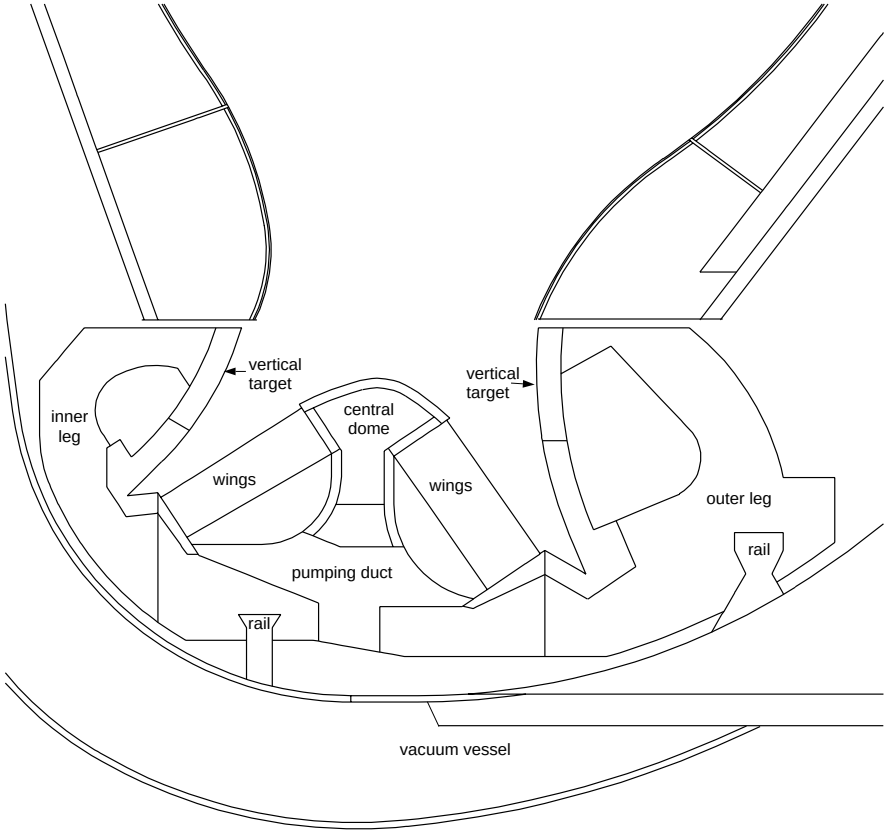

Fig. 1. Vertical cross section at the middle of the cassette model.

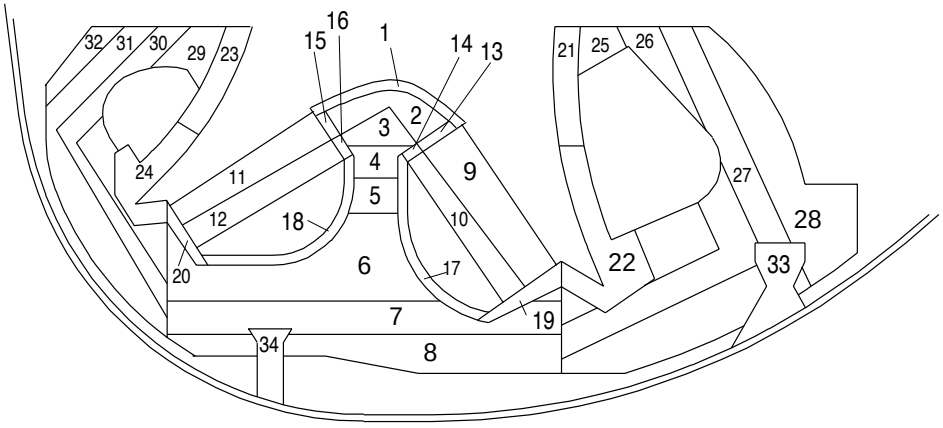

Fig. 2. Vertical cross section in the cassette showing the cells used to determine the spatial variation of nuclear parameters.

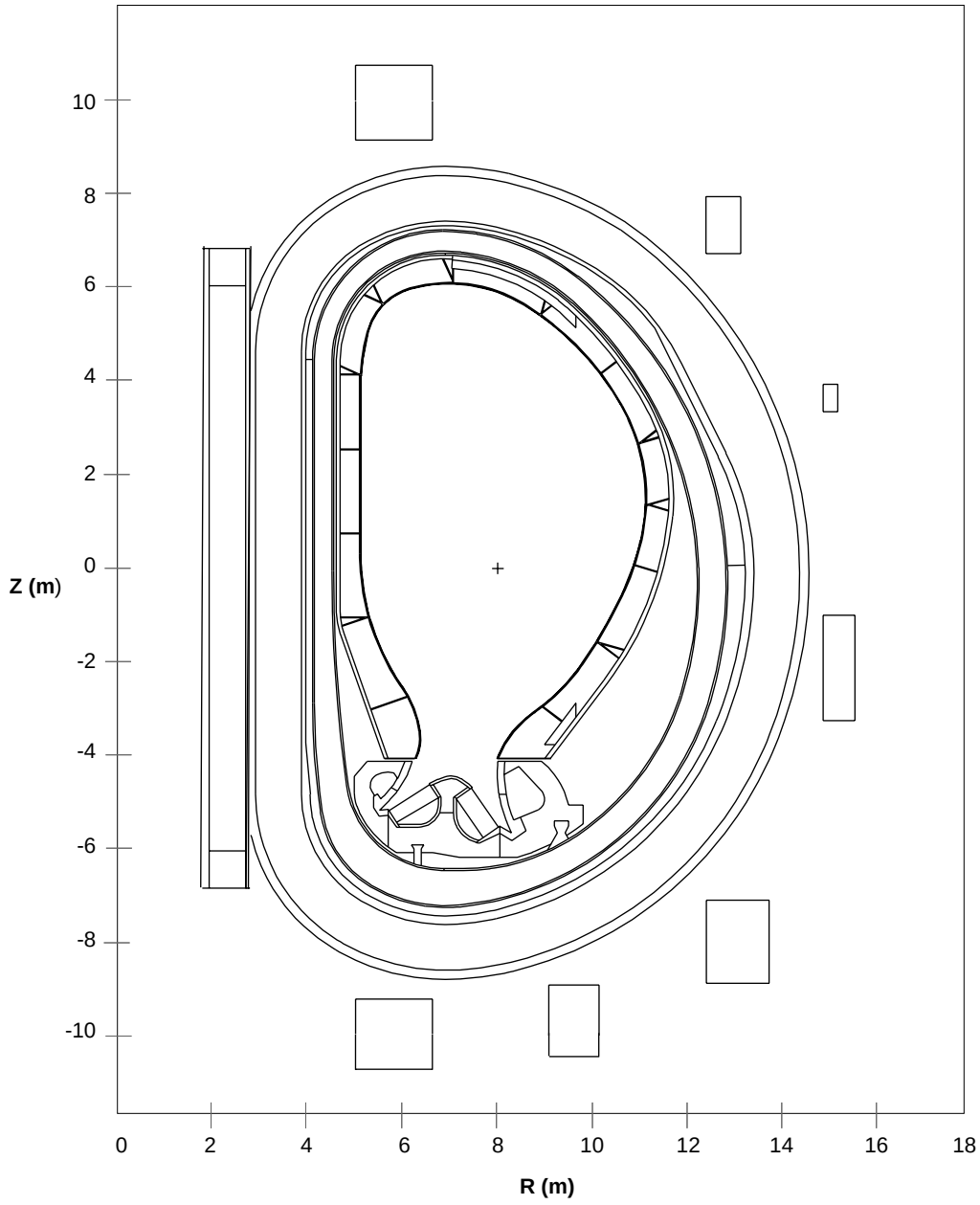

Fig. 3. Vertical cross section through the TF coils of the ITER 3-D model for MCNP calculations.

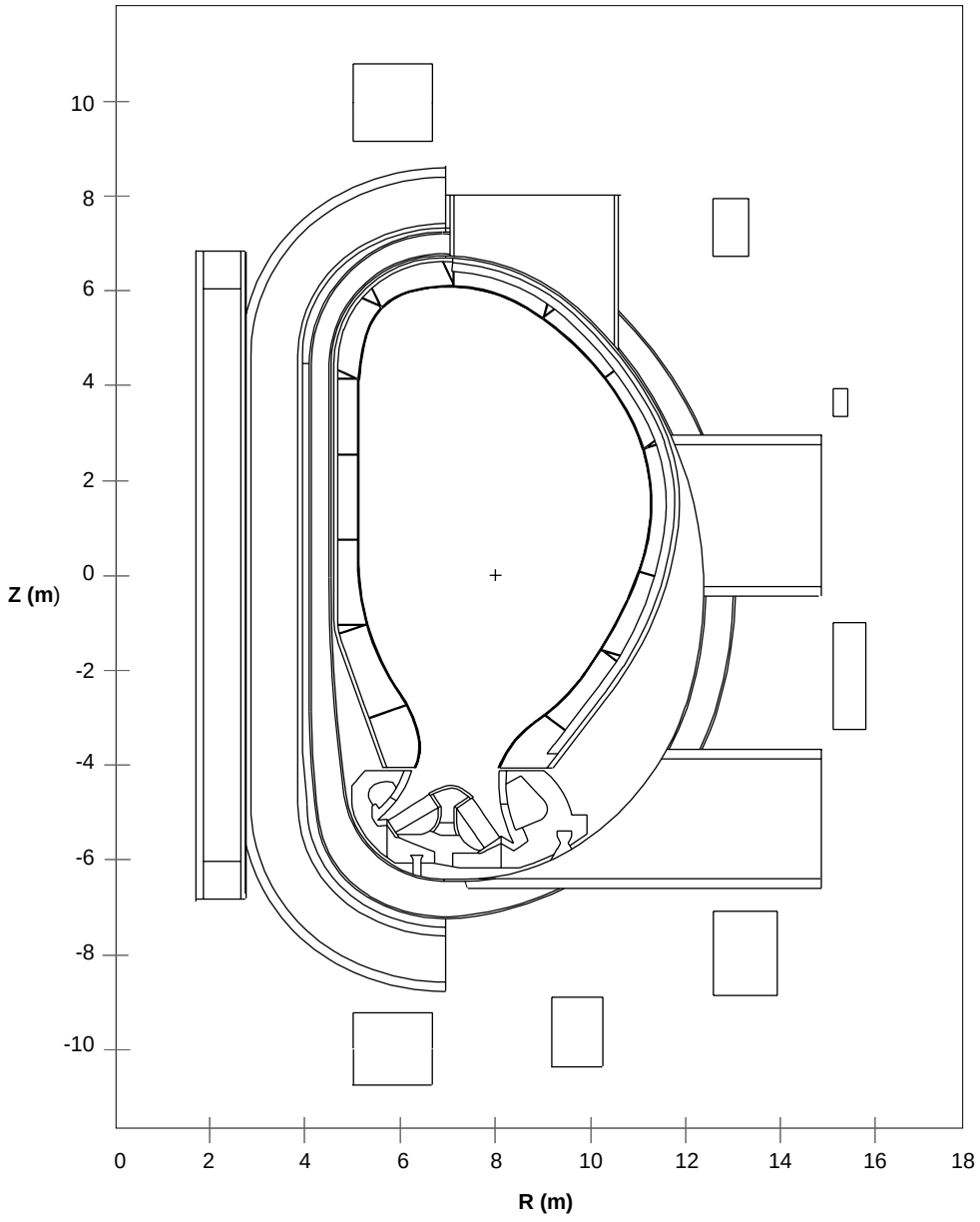

Fig. 4. Vertical cross section through the VV ports of the ITER 3-D model for MCNP calculations.

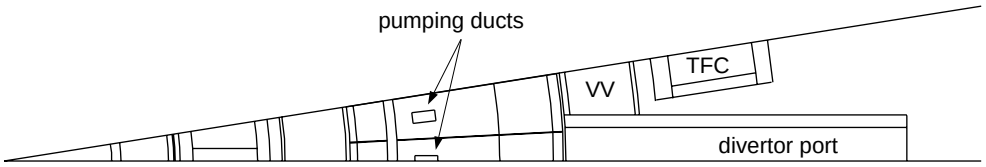

Fig. 5. Horizontal cross section of the 3-D model at Z= -6 m.

tori. The model employs 417 geometrical cells. The volumes of the different cells and the areas of surfaces of interest have been determined stochastically by ray tracing. In this calculation, all cells are assumed to not include any material and the geometrical model has been sprayed by 10 million particles at random directions. This calculation serves also as a mean for geometry checking by making sure that each point in space belongs to one of the cells used in the model. This calculation provided a successful check for the geometrical model.

A source subroutine has been written to modify MCNP to sample source neutrons from the source distribution in the ITER plasma provided numerically by the San Diego JCT at 1600 mesh points. Surface flux tallies are used to determine the peak radiation effects at the front surfaces of the different components of the divertor cassette, VV and TF coil and cell flux and energy deposition tallies are used to determine the volume averaged parameters and total nuclear heating in the components of the divertor and TF coil. The appropriate material compositions are used for the different cells of the model. The VV consists of two 4 cm thick 316SS plates sandwiching a shielding region made of 60% 316SS and 40% water. The winding pack of the TF coil consists of 43.2% SS, 11.7% Cu, 2.9% Nb_3Sn, 7.4% bronze, 16.8% liquid He, and 18% insulator (epoxy with 70% R-glass). The material composition used for the divertor cassette is given in Table 1. The calculation has been performed using 100,000 source particles yielding statistical uncertainties less than 10% in the calculated nuclear responses at the locations of interest. The calculation used 32 hours of CPU time on a Cray-2. The results are normalized to the nominal fusion power of 1500 MW. The end of life fluence related radiation effects have been determined for 1 full power year (FPY) of operation.

Table 1. Material Composition

Dome PFC	14% W, 13% Cu, 29% SS, 44% water
Central Dome Body	80% SS, 20% water
Wings	16% W, 79% Cu, 5% water packing fraction: 21% outer, 26% inner
Gas Box Liners	8% W, 74% Cu, 18% water
Vertical Targets	top section: 7% W, 22% Cu, 52% SS, 19% water lower section: 17% C, 20% Cu, 46% SS, 17% water
Inner and Outer Legs	80% SS, 20% water
Rails	100% SS

3. Neutron Wall Loading Distribution

The poloidal distribution of the neutron wall loading in the different regions of ITER has been determined using MCNP. In this calculation, only the uncollided neutron current crossing the first wall and the front surface of the divertor cassette is tallied. Two million source particles have been sampled in the MCNP calculation yielding statistical uncertainty less than 0.5% in the calculated wall loading. Source particles travel through void in the plasma chamber until they cross the wall. Particles are killed upon crossing the wall. Surface current tallies have been determined by counting particles crossing the wall. The first wall surface has been segmented into 53 poloidal segments and particles crossing each segment have been tallied. The plasma facing surface of the divertor cassette has been segmented into 21 poloidal segments to provide the neutron wall loading distribution in the divertor region. The length of each segment is less than 0.5 m. The exact segment areas were calculated analytically. The peak inboard and outboard wall loadings are 0.95 and 1.25 MW/m^2, respectively. The average values in the inboard and outboard regions are 0.69 and 1.06 MW/m^2, respectively. Figure 6 gives the poloidal variation of neutron wall loading in the divertor as a function of toroidal length measured in the counter-clockwise direction from the upper corner of the inner vertical target. The neutron wall loading peaks at 0.56 MW/m^2 in the central dome which has the largest view of the plasma. The plasma view factor for the inner vertical target is very small resulting in very low neutron wall loading. The average neutron wall loading in the divertor cassette is 0.16 MW/m^2.

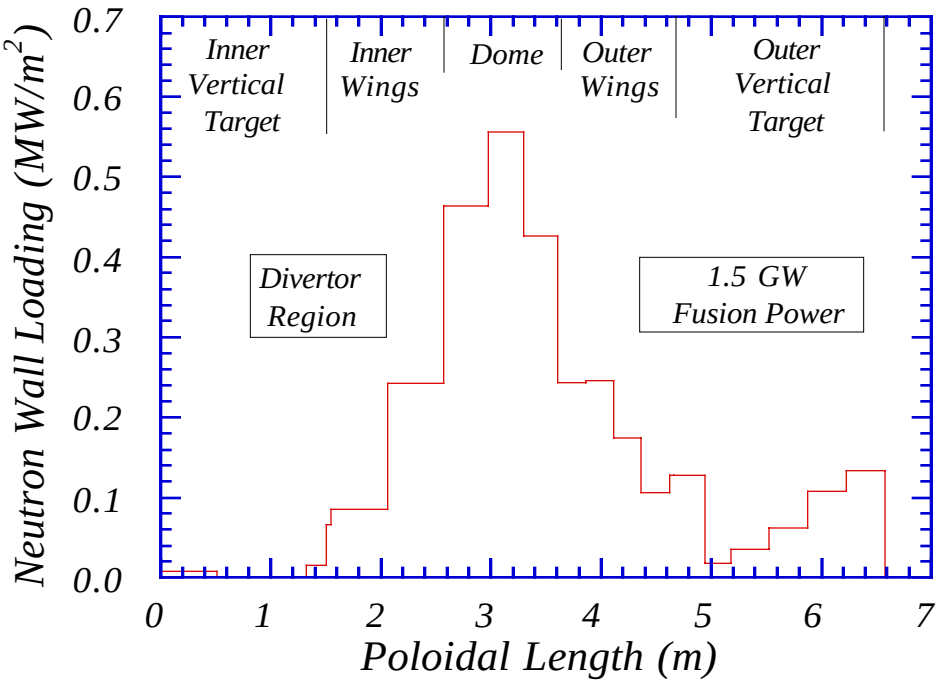

Fig. 6. Poloidal neutron wall loading distribution in the divertor.

4. Nuclear Parameters in the Divertor Cassette

The neutronics parameters have been calculated in the different components of the divertor cassette. These parameters included nuclear heating, atomic displacement and helium production. The radiation damage was calculated for both stainless steel and copper structures. The volume averaged parameters were determined for 32 segments of the cassette using cell flux and energy deposition tallies. These results are given in Table 2. The zone numbers correspond to the numbers given in Fig. 2. The peak nuclear responses were determined also at the front surfaces of the cassette components using surface flux tallies. These are given in Table 3. The largest heating and damage occurs in the dome PFC which has a full view of the plasma and has the largest neutron wall loading. The vertical targets and wings experience moderate levels of heating and damage with these values dropping rapidly as one moves deeper in the cassette body. For example, nuclear heating in the outer rail is only 2.9×10^{-4} W/cm^3 and the dpa and helium

Table 2. Spatial Distribution of Nuclear Responses in the Divertor Cassette

Zone Number	Power Density (W/cm^3)	dpa in SS (dpa/FPY)	dpa in Cu (dpa/FPY)	He Prod. in SS (appm/FPY)	He Prod. in Cu (appm/FPY)
Dome PFC					
1	7.56	3.08	3.27	60.73	31.91
Dome and Central Body					
2	2.37	1.06	1.09	19.31	8.42
3	6.29e-1	1.82e-1	2.01e-1	3.80	1.02
4	2.12e-1	4.80e-2	5.20e-2	1.62	2.33e-1
5	1.85e-1	3.54e-2	3.84e-2	1.33	1.33e-1
6	1.66e-1	4.60e-2	5.24e-2	1.25	2.48e-1
7	1.17e-1	3.33e-2	3.53e-2	8.64e-1	1.72e-1
8	3.21e-2	7.69e-3	8.88e-3	2.33e-1	3.63e-2
Wings					
9	3.17	1.46	1.50	19.52	13.42
10	1.15	5.50e-1	5.76e-1	5.29	3.48
11	2.86	1.42	1.50	18.82	12.51
12	1.12	5.61e-1	5.91e-1	5.67	3.78
Gas Box and Wing Plates					
13	2.14	7.46e-1	7.59e-1	10.61	4.39
14	8.85e-1	2.06e-1	2.19e-1	3.52	1.01
15	2.14	7.51e-1	7.93e-1	12.06	6.47
16	6.88e-1	1.84e-1	1.95e-1	2.39	6.45e-1
17	6.21e-1	2.01e-1	2.11e-1	2.55	9.82e-1
18	5.61e-1	1.78e-1	1.83e-1	2.18	8.32e-1
19	1.31	5.59e-1	5.77e-1	7.91	4.38
20	7.26e-1	2.50e-1	2.63e-1	3.76	1.78
Vertical Targets					
21	2.17	7.39e-1	7.71e-1	12.31	5.62
22	9.22e-1	3.36e-1	3.52e-1	8.26	2.47
23	1.30	2.97e-1	3.12e-1	4.68	5.52e-1
24	5.19e-1	1.38e-1	1.44e-1	4.17	4.87e-1
Outer Leg					
25	1.77e-1	4.49e-2	4.87e-2	1.24	2.51e-1
26	7.41e-2	1.66e-2	1.79e-2	4.63e-1	7.27e-2
27	2.36e-2	3.84e-3	4.30e-3	1.52e-1	1.23e-2
28	4.71e-3	7.88e-4	8.95e-4	3.05e-2	2.53e-3
Inner Leg					
29	1.30e-1	2.65e-2	2.91e-2	8.26e-1	9.12e-2
30	5.38e-2	8.17e-3	8.88e-3	3.22e-1	3.11e-2
31	1.06e-2	1.62e-3	1.80e-3	6.73e-2	4.25e-3
32	7.22e-3	9.20e-4	9.81e-4	5.02e-2	3.10e-3
Rails					
33	2.89e-4	6.33e-5	8.93e-5	1.26e-3	9.25e-5
34	4.92e-3	1.91e-3	2.38e-3	1.90e-2	1.83e-3

Table 3. Peak Nuclear Responses in the Divertor Cassette

	Power Density (W/cm^3)	dpa (dpa/FPY)	He Production (appm/FPY)
Dome PFC	10.75	4.69 SS 5.04 Cu	89.16 SS 55.39 Cu
Central Dome Body	5.39	2.28 SS	40.22 SS
Outer Wings	7.34	2.98 Cu	31.26 Cu
Inner Wings	5.79	2.17 Cu	20.40 Cu
Outer Vertical Target	5.46	2.60 SS 2.77 Cu	46.54 SS 26.29 Cu
Inner Vertical Target	3.72	0.95 SS 0.98 Cu	18.31 SS 11.95 Cu

production values are 6.3×10^{-5} dpa/FPY and 1.3×10^{-3} He appm/FPY. In general, the nuclear parameters in the inboard side of the cassette are lower than those in the outboard side that has a larger view of the plasma. Atomic displacements in Cu are slightly higher than in SS while helium production is much lower because of the higher gas threshold energy of nuclear reactions producing helium. The nuclear heating map in the cassette is given in Fig. 7 based on the 3-D results. Table 4 gives the total amount of nuclear heating for each of the zones used in the MCNP calculation. The total nuclear heating has been calculated for the 60 divertor cassettes to be 102.4 MW. The major contributors are the outer vertical target with 23.1 MW and the dome PFC with 19.7 MW.

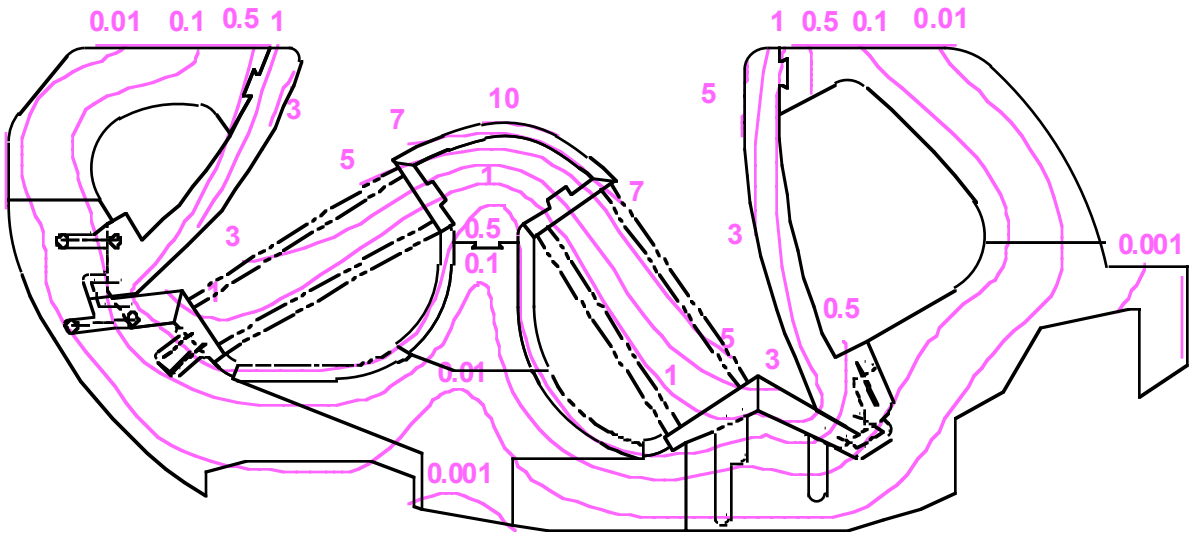

Fig. 7. Nuclear heating (W/cm^3) map in the divertor cassette.

Table 4. Total Nuclear Heating in the 60 Divertor Cassettes

Zone Number	Power Density (W/cm^3)	Volume per cassette (cm^3)	Total nuclear heating in 60 cassettes (MW)
Dome PFC			
1	7.56	4.35e4	19.732
Dome and Central Body			
2	2.37	8.15e4	11.589
3	6.29e-1	4.64e4	1.751
4	2.12e-1	3.93e4	0.500
5	1.85e-1	4.02e4	0.446
6	1.66e-1	2.91e5	2.898
7	1.17e-1	2.81e5	1.973
8	3.21e-2	2.77e5	0.534
Wings			
9	3.17	4.28e4	8.141
10	1.15	2.30e4	1.587
11	2.86	2.90e4	4.976
12	1.12	2.70e4	1.814
Gas Box and Wing Plates			
13	2.14	1.07e4	1.374
14	8.85e-1	4.76e3	0.253
15	2.14	7.54e3	0.968
16	6.88e-1	6.54e3	0.270
17	6.21e-1	4.86e4	1.811
18	5.61e-1	4.49e4	1.511
19	1.31	3.94e4	3.097
20	7.26e-1	1.44e4	0.627
Vertical Targets			
21	2.17	8.81e4	11.471
22	9.22e-1	2.10e5	11.617
23	1.30	6.34e4	4.945
24	5.19e-1	8.41e4	2.619
Outer Leg			
25	1.77e-1	1.94e5	2.060
26	7.41e-2	3.68e5	1.636
27	2.36e-2	5.32e5	0.753
28	4.71e-3	4.35e5	0.123
Inner Leg			
29	1.30e-1	1.06e5	0.827
30	5.38e-2	1.14e5	0.368
31	1.06e-2	1.97e5	0.125
32	7.22e-3	3.76e4	0.016
Rails			
33	2.89e-4	1.36e5	0.002
34	4.92e-3	4.82e4	0.014
Total		4.01e6	102.43

5. Nuclear Parameters in Vacuum Vessel

Streaming through the pumping ducts in the bottom of the cassette can result in damage hot spots in the VV behind it. The impact of neutron streaming through the ducts was analyzed for previous designs and recommendations regarding their configuration and size were made to minimize nuclear heating and helium production in parts of the VV behind them. In the interim design considered here, the pumping ducts are more inclined towards the outer and inner divertor legs such that the VV behind them does not see any direct neutrons from the plasma. This helps cut down the He production which is critical for rewelding. Only low energy secondary neutrons stream through the pumping ducts. The VV results were determined both for toroidal locations away from the ducts and behind the ducts by segmenting the front surface of the VV below the cassette. The results are given in Table 5. A peaking factor of about 5 results from streaming through the ducts. The peak helium production value of about 0.5 He appm/FPY indicates that rewelding of parts of the VV behind the pumping ducts might be feasible. Since these areas of relatively high helium production are very small, the design of the VV can locate the welds away from streaming path if these values are of concern for rewelding. Another area of concern for rewelding is the divertor port where relatively high damage is expected due to neutron streaming. The helium production was calculated along the divertor port. The largest damage occurs at the location where the port wall joins to the front VV wall and drops as one moves along the port away from the plasma chamber. The peak helium production is 0.036 appm/FPY and drops to 0.005 appm/FPY at locations adjacent to the back of the TF coil. It is clear from these results that rewelding of the divertor port is feasible.

Table 5. Peak Nuclear Responses in the VV behind the Divertor Cassette

	Power Density (W/cm^3)	dpa (dpa/FPY)	He Production (appm/FPY)
Behind pumping duct	0.034	0.025	0.48
Behind cassette body	0.018	0.005	0.09

6. Magnet Radiation Effects in the Divertor Region

The peak magnet radiation effects have been calculated in segments of the TF coils adjacent to the divertor port, between the divertor port and the horizontal port, and behind the divertor cassette below the divertor port. The radiation effects at the front surface of the TF coils adjacent to the divertor port are about an order of magnitude higher than those above and below the port due to radiation streaming through the port as illustrated by the results in Table 6. Table 7 gives the magnet radiation effects in the part of the TF coil adjacent to the divertor port. The results are given at the front and side surfaces of the coil. The radiation effects are higher at the side surface due to the effect of streaming. The calculated radiation effects are much lower than the radiation limits considered in ITER. These radiation limits are 2 and 1 kW/m^3 for the coil case and winding pack power density, respectively, and 1×10^9 rads for the end-of-life insulator dose [3]. Although no limits were specified for fast neutron fluence and Cu dpa in the EDA, the results are about three orders of magnitude lower than the limits of 1×10^{19} n/cm^2 and 6×10^{-3} dpa used in the CDA [4]. It is clear that the sides of the TF coils are well protected from radiation streaming into the divertor ports.

The total nuclear heating in the parts of the 20 TF coils in the divertor region is given in Table 8. The results are given for the front, back, and side coil cases as well as the winding pack. The total nuclear heating is 2.081 kW with 1.575 kW contributed by the parts adjacent to the divertor port. The statistical uncertainty is less than 5%. The heating in the part below the port

Table 6. Magnet Radiation Effects at Front Surface of the TF Coils in the Divertor Region

	Above Divertor Port	Adjacent to Divertor Port	Below Divertor Port
Coil case power density (kW/m^3)	6.87×10^{-3}	0.080	7.62×10^{-3}
Winding pack power density (kW/m^3)	3.01×10^{-4}	5.12×10^{-3}	3.80×10^{-4}
Insulator dose (Rad/FPY)	4.18×10^5	4.46×10^6	3.64×10^5
Fast neutron fluence (n/cm^2 per FPY)	4.98×10^{14}	6.27×10^{15}	5.28×10^{15}
Copper dpa (dpa/FPY)	3.11×10^{-7}	2.38×10^{-6}	2.29×10^{-7}

Table 7. Magnet Radiation Effects at Front and Side Surfaces of the TF Coils Adjacent to the Divertor Port

	Front surface	Side surface
Coil case power density (kW/m^3)	0.080	0.126
Winding pack power density (kW/m^3)	5.12×10^{-3}	6.38×10^{-3}
Insulator dose (Rad/FPY)	4.46×10^{6}	6.78×10^{6}
Fast neutron fluence (n/cm^2 per FPY)	6.27×10^{15}	1.10×10^{16}
Copper dpa (dpa/FPY)	2.38×10^{-6}	4.46×10^{-6}

Table 8. Total Nuclear Heating (kW) in the TF Coils in the Divertor Region

	Above Divertor Port	Adjacent to Divertor Port	Below Divertor Port
Inner case	0.031	0.409	0.036
Outer case	0.005	0.114	0.075
Side case	0.035	0.868	0.249
Winding pack	0.009	0.185	0.065
Total	0.080	1.576	0.425

is about a factor of 5 more than that in the part above the port. Only 0.03 kW is contributed by the inboard parts of the TF coils behind the divertor cassette. The total nuclear heating in the TF coils should not exceed 17 kW. It is essential to determine the additional heating in the other parts of the coils and add them to the contribution from the divertor region to determine whether the total heating limit can be satisfied.

It is interesting to note that the results in the winding pack are lower than those in the outline design [5] where additional shielding was provided by the 11 cm support structure between the divertor port and the TF coil. This is attributed partly to the added attenuation in the 20 cm coil case that was not used in the outline design. Furthermore, the present interim design has a thicker outer divertor leg of 48 to 100 cm in addition to the 15 cm thick vertical target compared to a total thickness of only 45 cm in the previous outline design. Also the baffle on the outboard side is more than 1 m thick compared to an 80 cm thick blanket in the previous design. In addition, the pumping ducts in the cassette are pointing downward while they were in the outer leg and pointing directly towards the port in the previous design. These differences result

in less streaming into the port and compensate for the loss of the additional 11 cm shielding taken credit for in the previous design.

7. Summary and Conclusions

3-D neutronics and shielding analyses have been performed for the divertor region. A detailed 3-D model has been developed for the ITER interim design. The model includes the first wall, blanket modules, back plate, coolant manifolds, VV with major ports, divertor cassettes, TF coils and PF coils. The source neutrons are sampled from the source distribution in the ITER plasma. The poloidal distribution of the neutron wall loading in the different regions of ITER has been determined using MCNP. For the nominal 1500 MW fusion power, the peak neutron wall loading in the divertor region is 0.6 MW/m^2 at the divertor cassette dome.

The spatial distribution of the neutronics parameters has been determined in the different components of the divertor cassette. The total nuclear heating has been calculated for the 60 divertor cassettes to be 102.4 MW. The peak helium production in the VV behind the pumping ducts is 0.5 He appm/FPY implying that rewelding might be feasible. In addition, helium production in the divertor port wall is less than 0.04 He appm/FPY. The TF coils are well protected from radiation streaming into the divertor ports with the peak end-of-life insulator dose, neutron fluence, and Cu damage being well below the design limits. The total nuclear heating in the parts of the TF coils in the divertor region is only 2.1 kW. Heating in the remainder of the coils including contribution from streaming in other major ports needs to be determined to calculate the total magnet heating.

References

[1] J. Briesmeister, Ed., "MCNP, A General Monte Carlo N-Particle Transport Code, Version 4A," LA-12625-M (1993).

[2] R. MacFarlane, "FENDL/MC-1.0, Library of Continuous Energy Cross Sections in ACE Format for MCNP-4A," Summary Documentation by A. Pashchenko, H. Wienke and S. Ganesan, Report IAEA-NDS-169, Rev. 3, International Atomic Energy Agency (Nov. 1995).

[3] ITER General Design Requirements, International Thermonuclear Experimental Reactor, 22 March 1996.

[4] ITER Conceptual Design Report, ITER Documentation Series no. 18, IAEA, Vienna, 1991.

[5] M. Sawan, Y. Gohar, and R. Santoro, "Shielding Analysis for the ITER Divertor and Vacuum Pumping Ducts," Fusion Engineering & Design 28, 429 (1995).